Procedure for identifying the thermal reaction of defects in solidified layers during the PBF-LB/M process using active thermography

Fabian Herzer, Johannes Rau, Christian Seidel, Johannes Schilp

Angaben zur Veröffentlichung / Publication details:

Herzer, Fabian, Johannes Rau, Christian Seidel, and Johannes Schilp. 2023. "Procedure for identifying the thermal reaction of defects in solidified layers during the PBF-LB/M process using active thermography." *Procedia CIRP* 118: 670–75. https://doi.org/10.1016/j.procir.2023.06.115.

Available online at www.sciencedirect.com

ScienceDirect

Procedia CIRP 118 (2023) 670–675

www.elsevier.com/locate/procedia

16th CIRP Conference on Intelligent Computation in Manufacturing Engineering, CIRP ICME '22, Italy

Procedure for Identifying the Thermal Reaction of Defects in Solidified Layers during the PBF-LB/M Process using Active Thermography

Fabian Herzer[a,*], Johannes Rau[a], Christian Seidel[a,b], Johannes Schilp[a,c]

[a]*Fraunhofer IGCV (Institute for Casting, Composite and Processing Technology), Am Technologiezentrum 10, 86159 Augsburg, Germany*
[b]*Department of Applied Siences and Mechatronics, University of Applied Siences Munich, Lothstr. 34, 80335 Munich, Germany*
[c]*University of Augsburg, Chair of Digital Manufacturing, Faculty of Applied Computer Sience, Eichleitnerstr. 30, 86159 Augsburg, Germany*

* Corresponding author. Tel.: +49 821 90678-186; fax: +49 821 90678-199. *E-mail address:* fabian.herzer@igcv.fraunhofer.de

Abstract

The geometrical complexity of additively manufactured parts and the comparatively high densities of the metallic materials used mean that non-destructive testing technologies reach their limits when it comes to post-process testing. In order to still be able to ensure the quality of parts the inspection must be implemented into the build-up process. A suitable technology for this is active thermography, as it can detect defects close to the surface and can use the laser of the manufacturing machine as an excitation source. In this paper, a procedure to identify the thermal reactions of defects in solidified layers and the results for the material 1.4404 are presented.

Keywords: PBF-LB/M; Lack of fusion; Active thermography; Process monitoring; Defects; Defect categories

1. Introduction

The additive manufacturing industry has grown strongly in the past decade. Even in times of the Covid-19 pandemic, it was able to record growth of around 7.5 percent, although one of the central industries of additive manufacturing, aerospace, suffered from the economic consequences of the pandemic. [2] Nevertheless, AM in aviation is expected to recover quickly in the coming years. [3]

For this to succeed and for additive manufacturing processes to be used increasingly in the production of aerospace components, solutions must be found to the current challenges in the areas of quality assurance and certification. [3] However, these topics do not only represent one of the central challenges for the aerospace sector, but are generally considered to be an obstacle in the field of the application of additive manufacturing processes. [2, 4] Surveys and interviews conducted by the Fraunhofer-Gesellschaft revealed that 95 % of respondents considered these topics to be relevant for the implementation of their business model. For 53 % of the respondents, it was even very important and only cost reduction was ranked higher. [4]

The reasons why the topics of quality assurance and certification continue to pose major challenges are the complexity of the components or the materials used and the interpretability of the data. Non-destructive testing techniques reach their limits when inspecting already completely manufactured components for structural defects such as pores, cracks, delaminations or binding defects [5–7]. Due to the complexity of the parts, techniques such as ultrasound, eddy current or optically excited thermography cannot couple their test medium into the component. [5, 6, 8] Computed tomography is currently the most commonly used testing technology. It is also suitable for complex structures due to the contactless inspection. Nevertheless, this technology is also limited. Depending on the material used, the resolution is insufficient due to the material density and only very small components can be inspected for defects or lack of fusion defects cannot be detected. Another disadvantage is the high time and cost expenditure. A 100 % inspection is therefore not economical for larger quantities or components. [9]

10.1016/j.procir.2023.06.115

Process monitoring methods are used to circumvent these problems. The approach is to detect the microstructural defects directly as they occur. Due to the layered structure of the build-up-process in powder bed-based melting of metals by means of a laser beam (PBF-LB/M), the component complexity plays a subordinate role in this approach as quality is assured layer-by-layer. Technologies are used here that detect and interpret the process emissions in the form of radiation or sound.

The interpretation of the data is the biggest challenge. Due to the large number of influencing factors, it is very difficult to establish a cause-effect relationship. In addition, these approaches usually consider the melt pool and thus the layer formation process. It is challenging to predict whether defects will develop in the component and how they will be changed by the subsequent layers. Within this contribution, an approach is therefore introduced that uses active thermography to examine already solidified layers for bonding defects in order to circumvent these uncertainties.

2. State of the art

As already mentioned, there are different types of structural defects caused by PBF-LB/M. Why the lack of fusion defects in particular are suitable for detection by means of active thermography and what approaches exist for in-situ process monitoring by means of thermography is described in the following section.

2.1. Lack of fusion defects

Lack of fusion defects are characterised as localised interruptions in the bonding of two layers. These are mainly caused by an insufficient energy input. This can be caused, for example, by a drop in laser power, defocusing of the laser, e.g. due to process smoke [10], balling [11] or excessive layer thickness. If the energy input is too low, the required melt pool depth will not be reached. This results in an insufficient overlap between the layers. Un-melted powder between the scan tracks is the result, which is difficult to melt after applying the next layer. The consequence are incomplete fusion holes that remain in the part. Because of this, lack of fusion defects are generally located between layers. [1, 12, 13]

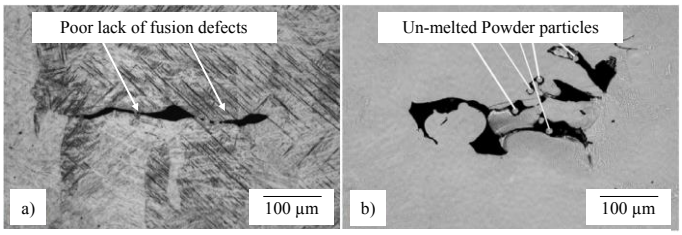

Fig. 1. Types of lack of fusion defects, a) bonding between two layers filled with process gas, b) lack of fusion defects with unmelted powder particles [13].

As can be seen in Figure 1, binding defects can generally be divided into two categories. Category 1: Hollow lack of fusion defects in which the process gas is trapped. Category 2: lack of fusion defects which contain un-melted powder particles. [1] Due to the formation between the layers and sizes of up to several 100 µm [10], these defects are suitable for detection by thermography. In order to be detected by active thermography, the defects must fulfil the following law:

$$Minimum\ detectable\ Defect\ size \geq Defect\ depth \quad (1)$$

With layer thicknesses of 30 - 50 µm, lack of fusion defects can thus be detected several layers deep. If they are outside the reach of the melting depth, they are not further changed by the process and remain in the component. Active thermography therefore offers high potential to detect them during the build process.

Other defects such as pores or cracks are usually too small and do not form exclusively parallel to the surface [14, 15]. Detection by thermography is therefore unlikely, which is why only the lack of fusion defects are considered in this work.

2.2. Thermography

Thermography is generally the non-contact detection, processing and visual display of the distribution of thermal radiation emanating from an object that can be detected with an IR detector system [16]. If it is used for the purpose of non-destructive testing of components, a distinction is made between passive and active thermography.

2.2.1. Passive vs. Active approach

Passive thermography uses only the heat flux generated by the intrinsic heat of the test object. This heat consists of both internally generated heat and heat applied externally (e.g. in an oven). Passive thermography is used, for example, in buildings (e.g. to detect moisture, thermal bridges, leaks), to inspect electrical or mechanical equipment and in process and plant diagnostics. [17]

Active thermography is used when components in industrial production are inspected for near-surface imperfections or defects. For the purpose of the inspection, a transient heat flow is generated by an external energy source in the test object and the behaviour of the component in response to this excitation is recorded using infrared cameras. Depending on the defect to be detected, different excitation sources can be used. They differ significantly in the form of their temporal excitation signal. [17] In Figure 2 the differences in the heat flow of these two approaches are shown:

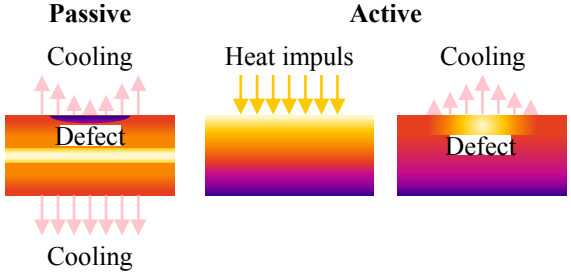

Fig. 2. Heat flow passive and active approach.

In addition to flash or halogen lamps, ultrasound and induction, a laser can also be used to generate the transient heat flow. PBF-LB/M machines therefore already have an internal excitation source. By scanning the component vector-wise, it is only heated locally for a short time, which corresponds to a

quasi-pulse excitation. In the context of this work, the laser is therefore used as an external excitation source.

2.2.2. In-situ Thermography approaches in AM

Looking at the state of research, active thermography has so far only been used in the post-process as a non-destructive testing method [18]. There are also approaches investigating in-situ use by means of flash lamps, but these have not yet passed the laboratory stage and have not yet been implemented in a PBF-LB/M system [19].

In contrast to the active approach, which has been little used to date, the use of passive in-situ thermography is already more widespread. The objects of observation range from the recording of melt pool temperatures [20] or the temperature profile of the scan track [21] to the identification of melt pool ejections such as spatter [22].

In summary, none of the approaches addresses the defect detection of lack of fusion defects in already solidified layers by means of active thermography.

3. Experimental methods

To determine which thermal response to excitation by the system laser is caused by lack of fusion defects, this chapter presents the integration of thermography into a PBF-LB/M system and a method to verify the response.

3.1. Integration of the Thermography-System

All experiments were performed on an AconityOne machine (Aconity, Aachen (Germany)). A module was developed and implemented for the off-axis integration of the thermography camera. This module makes it possible to keep the camera's angle of view as steep as possible at 65° and thus keep the distortion as low as possible. On the camera technology side, quantum detector cameras of the type FLIR X8400sc and IRCAM Equus327k SM were used. These are both sensitive in the MWIR range (2.5 - 5.1 µm) and have split-image detectors (FLIR 1.280 x 1.028 Px, IRCAM 640 x 512 Px), allowing frame rates of several hundred Hertz to be generated.

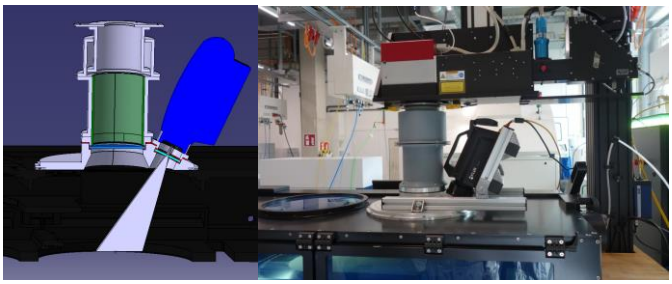

Fig. 3. Integration of the thermography camera (CAD-model (left), implementation in the AconityOne machine (right).

By tapping the TTL signals that the system controller passes to the scanner card of the laser, it was possible to synchronize the image acquisition of the cameras with the layer excitation of the AconityOne.

3.2. Procedure

The following steps were defined in order to be able to assign the recorded reaction behavior of the laser excited solidified layers to the causes.

3.2.1. Artificial insertion of defects

The artificial introduction of the lack of fusion defects was carried out according to [23]. For this purpose, cavities of predefined sizes are provided in the CAD model of the component. They thus fulfill the criteria “fixed position”, “realistic” and “existing”.

3.2.2. Analysis of the thermographic reaction

This step includes the manual identification of hotspots. For this purpose, the laser path during excitation is observed within

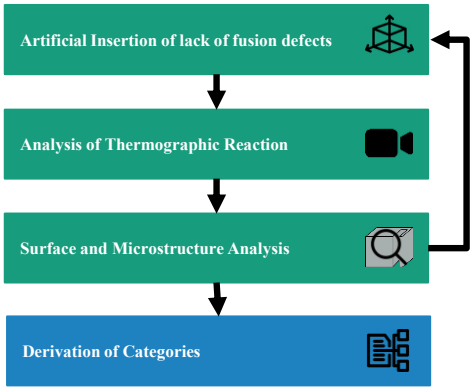

Fig. 4. Procedure to link reactions with causes.

the image sequence. If a hotspot is formed after a laser passed an area on the surface, the intensity of the hotspot as well as a defect-free area is detected by means of region of interest (ROIs). The difference between these values is referred to as contrast in the following.

3.2.3. Analysis of the surface and microstructure

In order to be able to identify the causes of hotspots, this step involves examining the surface by means of laser microscopy on the one hand and the microstructure of the component by means of micrographs or CT scans on the other. Based on the laser microscope images, it can be deduced whether the hotspots in the thermograms are caused by abnormalities on the surface. By means of the microsections or the CT scans, the size and depth of the introduced defects can be determined and thus the detectability can be verified according to the physical law mentioned in 2.1.

3.2.4. Derivation of categories

In the last step, the collected information of the individual investigation steps is combined and compared with each other. The following characteristics were defined for distinguishing the individual categories:

- Response area: this is the area of the detector in pixels that is excited with the detected intensities when the defect area is excited.
- Intensity: The intensity is measured in comparison to defect-free areas of the components.
- Reaction time: this refers to the time period during which a structure causes a hotspot in response to laser excitation. It is determined by the number of recorded images as well as the integration time in which the hotspots can be seen within the image sequence.
- Spatter occurrence: This is determined when, in addition to the stationary hotspot, other moving hotspots occur

- Cause: The possible cause is derived from the laser microscope images and is placed in context with the expressions of the other features.

The procedure is shown in Figure 4. The first three steps have to be repeated to get enough information, because after printing and capturing the thermographic reaction of a defect, the part must be taken out of the machine for the surface and microstructure analysis.

4. Case study

This chapter shows the result applying the procedure on the material 1.4404. For the build-up of the defect samples standard parameters were used (214 W laser power, 928 mm/s scan speed, 0.1 mm hatch space and a layer thickness of 0.04 mm). In order to be able to test the reaction behaviour in both simple and complex structures, the component geometry from [23] was modified. As it can be seen in the following figure, the rectangle was extended by a thin bar for this purpose (width 1.4 mm).

The parameters already identified in preliminary work were used to excite the analysis layer: 70 W, 5.000 mm/s scanning speed, 0.1 mm hatch spacing. The hatches were exposed unidirectional. In order to prevent temperature peaks by exposing directly adjacent hatches, an artificial jumping of the hatches was realised. As can be seen in Figure 5, the hatches were divided into four blocks, each offset by one hatch and containing only every fourth hatch.

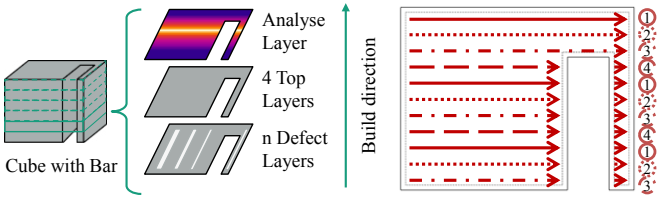

Fig. 6. Test geometry, stack structure and excitation strategy.

Since powder residues remain on the solidified layer after exposure to light, smoothing with upskin parameters must be carried out before performing the excitation for thermographic testing. This significantly reduces the amount of residual powder and the probability of hotspots triggered by this.

4.1.1. Artificial insertion of defects

The insertion of the artificial defects was performed as described in [23]. The difference to the previous work consists in adjusted defect dimensions. The reason for the adjustment was the need to further increase the resulting defect sizes to obtain more detectable defects according to (1). To investigate this, the defect heights were varied between 4, 6 and 8 layers or 160 µm, 240 µm and 320 µm and sections were evaluated microscopically. This was carried out both with cube samples with several stacks, in order to be able to evaluate several defect layers with one section, and with single stack samples, in order to be able to determine the distance to the surface layer and thus the defect depth.

The analyses showed that defects with four layers were often healed by the process or only remained in the component with lengths and widths of a few µm. Defects with 6 or 8 layers, on the other hand, remained clearly visible in the part and most of them had the required size/depth ratio. Therefore, these defect depths were used in the further course of the investigations.

4.1.2. Analysis of the thermographic reaction

For the recording of the thermal reaction behaviour, the process was interrupted after the build-up of the defect and cover layers and switched from the build parameters to the excitation parameters for the analysis layer. By starting the excitation, a trigger signal in the form of the high edge of the system state "laser on" is transmitted to the camera and thus excitation and recording are synchronised. Subsequently, the recorded image sequences were manually analysed for hotspots. In order to better classify whether a hotspot was located directly above an inserted defect, a template of the defect layer image was created and placed over the thermogram.

The analysis showed the following characteristics for the

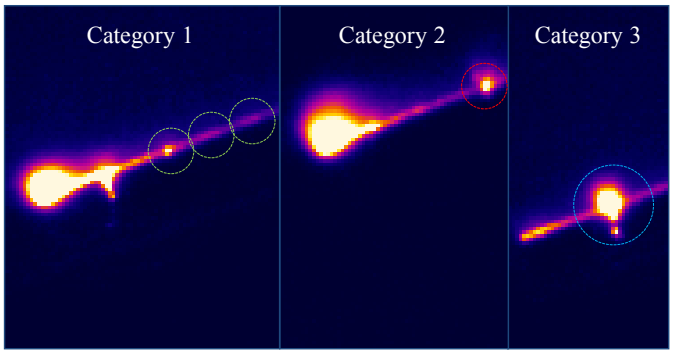

Fig. 5. Defect-categories with marked hotspots in the thermograms.

defined features:

- Response area: Here, a very large difference between the individual hotspots could be recognised. While some only appeared in a very small area (1 - 9 Px^2), there were also medium-sized (10 – 36 Px^2) and large hotspots (37 – 100 Px^2).
- Intensity: After determining the sizes, the intensity values were also examined with regard to the subdivisibility into the three categories. Comparative ROIs without increased intensity values were placed with the same number of pixels. This showed that there was a direct correlation with the sizes of the hotspots. Small hotspots produced contrasts between 30 and 200 DL, medium-sized ones between 800 and 2000 Dl and large ones between 5000 and 15000 DL.
- Reaction time: In the first step, two different reaction behaviours could generally be determined. There were hotspots, which were expressed in a period of 4 to 6 ms, thus immediately and only for a very short time after the excitation. There were also hotspots that appeared after 6 ms and for a significantly longer period of time up to 30 ms after the excitation.
- Spatter occurrence: In contrast to the other characteristics, this characteristic was not evaluated quantitatively, but qualitatively. It was determined that only the large hotspots of category

3 had spatters. This behaviour could not be found in the other two categories.

All results and the subdivision into the three defect categories can be seen in the table below:

Table 1. Identified characteristics of the defined features.

Category	Reaction Area (Px^2)	Intensity (DL)	Reaction time (ms)	Spatters
1	1 - 9	30 - 200	4 – 6	No
2	10 - 36	800 - 2000	6 – 20	No
3	37 - 100	5000 - 15000	6 – 30	Yes

4.1.3. Analysis of the surface and microstructure

The thermographic evaluation was followed by an examination of the surface or the microstructure in order to be able to link the reaction behaviour of the hotspots with possible causes.

First, the surface at the locations of the identified hotspots was examined for abnormalities using LSM. Exemplary results of these analyses can be seen in the following graphic:

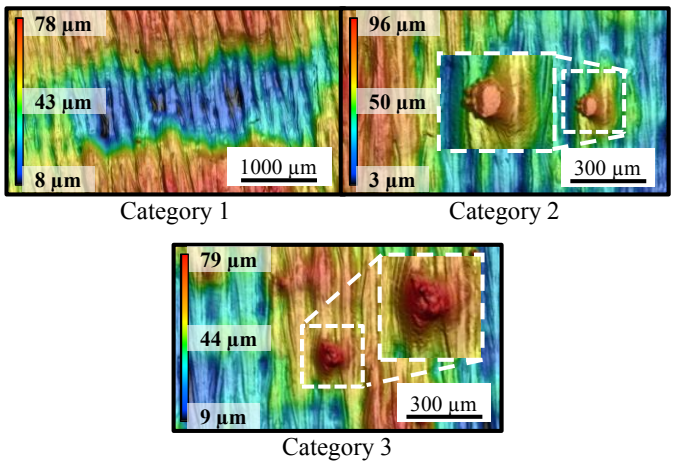

Figure 7: LSM images of the surface structure of the different hotspot categories

No particular anomalies were identified in category 1 hotspots. Although there were sinks at these locations caused by the defects that were introduced, these have no effect on the thermographic behaviour. An example of category 2 can be seen in Figure 8. The irregularity on the surface is approx. 100 x 100 µm wide and deep, and approx. 50 µm high. On closer inspection, it is noticeable that smaller spikes can be seen on the spherical top. These spikes could be satellites. This would mean that a loose powder particle was welded on. If it was pure balling, there would be no jagged edges on the tip. As can be seen (Category 3, Figure 8), there is a large irregularity on the surface. Due to the large area (124 x 126 µm) and the structure, which is not spherical but covered with peaks, balling can be neglected as a possible cause. Accordingly, it can be assumed that a large loose particle, which was only partially welded on, led to this unevenness. The measured height of approx. 30 µm is also smaller than that of the second type of unevenness, which is why it can be assumed that less material was transferred to the surface.

The last step in this procedure was to link the hotspots of category 1 with the presence of detectable lack of fusion defects. For this CT Scans were performed to verify, if the physical law (1) was fulfilled. In Figure 7 you can see artificial inserted lack of fusion defects of Category 1.

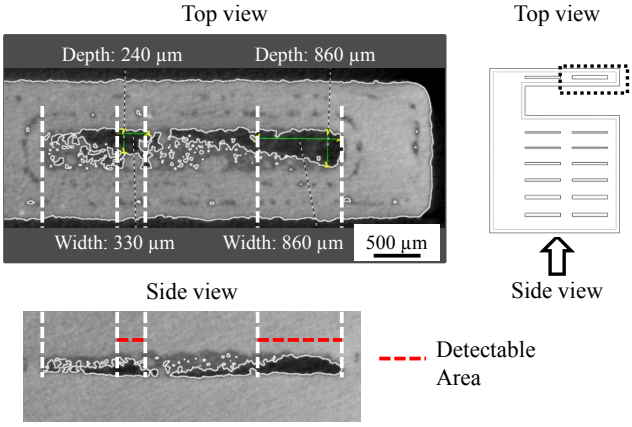

Fig. 8. CT scan of artificial inserted lack of fusion defects.

It can be seen, that the defects do not keep their original form of the CAD-Model. The resulting form is irregular and does not follow any pattern. This could be verified by building up defects with different shapes (e. g. ellipsoidal shape and different lengths and widths). This also explains why defects sometimes only get detected by one certain laser path. They not become visible when scanning the laser paths right next to it. The lower part of Figure 7 shows by means of red marking which areas have the necessary size-depth ratio and could thus be detected by thermography.

With this step, the hotspots of category 1 could thus be assigned their cause, lack of fusion defects. A summary of the categories and all their characteristics can be found in the Table 2.

5. Conclusion and outlook

Using the procedure presented, it was possible to define different defect categories for the material 1.4404 based on the characteristics time of occurrence, reaction area and surface condition. This makes it possible to assign occurring hotspots to the causes and to differentiate between lack of fusion defects and other imperfections. This is the basis for the design of the image processing for an automatic detection of lack of fusion defects, which is the next step of the project. Based on the

Table 2. Categorisation of detectable hotspots of solidified layers during the PBF-LB/M process using active thermography.

Category	Reaction Area (Px^2)	Intensity (DL)	Reaction time (ms)	Spatters	Cause
1	1 - 9	30 - 200	4 – 6	No	Lack of fusion defect
2	10 - 36	800 - 2000	6 – 20	No	Surface irregularity (e.g. Balling, small loose powder particles)
3	37 - 100	5000 - 15000	6 – 30	Yes	Surface irregularity (e.g. big small loose powder particles)

knowledge gained, framework conditions for data extraction from the laser path sequence can be derived. In the future, this should make it possible to generate individual images of the entire layer at a specific point in time from the recorded image sequence of the laser path.

Acknowledgements

The authors express their sincere thanks to the Land of Bavaria and its Bavarian Ministry of Economic Affairs, Regional Development and Energy StMWi for funding the "MULTIMATERIAL-Zentrum Augsburg" (English: "Multi-material Center Augsburg"). Furthermore, the authors thank Norbert Zimmer for the support while conducting the experiments.

References

[1] Q. C. Liu *et al.,* "The Effect of Manufacturing Defects on the Fatigue Behaviour of Ti-6Al-4V Specimens Fabricated Using Selective Laser Melting," *AMR*, 891-892, pp. 1519–1524, 2014.

[2] T. Wohlers *et al., Wohlers Report 2021: 3D Printing and Additive Manufacturing Global State of the Industry*. Fort Collins, Colo.: WOHLERS Associates, 2021.

[3] A. W. Khan, "Global Aerospace Additive Manufacturing Applications Growth Opportunities: Increased Technology Adoption and Materials Innovation Transforming Aerospace Parts Production," Global Aerospace & Defense Research Team at Frost & Sullivan, Santa Clara, USA, 2021.

[4] M. Basso *et al.,* "An Additive Manufacturing Breakthrough: A How-to Guide for Scaling and Overcoming Key Challenges," Whitepaper, World Economic Forum, Genf, Jan. 2022.

[5] S. Everton *et al.,* "Identification of Sub-Surface Defects in Parts Produced by Additive Manufacturing, Using Laser Generated Ultrasound," *Materials Science & Technology*, 2016.

[6] M. Grasso and B. M. Colosimo, "Process defects and in situ monitoring methods in metal powder bed fusion: a review," *Meas. Sci. Technol.*, vol. 28, no. 4, p. 44005, 2017.

[7] Y. Chen *et al.,* "Defect inspection technologies for additive manufacturing," *Int. J. Extrem. Manuf.*, vol. 3, no. 2, p. 22002, 2021.

[8] B. Dutton, M. H. Rosli, and D. Ross-Pinnock, "NDT Standards for Additive Manufacturing," Grenoble, Apr. 10 2018.

[9] D. Chauveau, "Review of NDT and process monitoring techniques usable to produce high-quality parts by welding or additive manufacturing," *Weld World*, vol. 62, no. 5, pp. 1097–1118, 2018.

[10] A. Ladewig *et al.,* "Influence of the shielding gas flow on the removal of process by-products in the selective laser melting process," *Additive Manufacturing*, vol. 10, pp. 1–9, 2016.

[11] F. Bayle and M. Doubenskaia, "Selective laser melting process monitoring with high speed infra-red camera and pyrometer," in *Proc. SPIE 6985: Fundamentals of Laser Assisted Micro- and Nanotechnologies*, Society of Photo-Optical Instrumentation Engineers (SPIE), Ed., 2008, 698505-698505-8.

[12] T. Vilaro, C. Colin, and J. D. Bartout, "As-Fabricated and Heat-Treated Microstructures of the Ti-6Al-4V Alloy Processed by Selective Laser Melting," *Metall and Mat Trans A*, vol. 42, no. 10, pp. 3190–3199, 2011.

[13] H. Gong *et al.,* "Analysis of defect generation in Ti–6Al–4V parts made using powder bed fusion additive manufacturing processes," *Additive Manufacturing*, 1-4, pp. 87–98, 2014.

[14] P. Mercelis and J. ‐ P. Kruth, "Residual stresses in selective laser sintering and selective laser melting," *Rapid Prototyping Journal*, vol. 12, no. 5, pp. 254–265, 2006.

[15] C. Weingarten *et al.,* "Formation and reduction of hydrogen porosity during selective laser melting of AlSi10Mg," *Journal of Materials Processing Technology*, vol. 221, no. 2, pp. 112–120, 2015.

[16] *Zerstörungsfreie Prüfung - Thermografische Prüfung - Teil 3: Begriffe; Deutsche Fassung EN 16714-3:2016*, DIN EN 16714-3, DIN Deutsches Institut für Normung e. V., Nov. 2016.

[17] *Zerstörungsfreie Prüfung - Thermografische Prüfung - Teil 1: Allgemeine Grundlagen; Deutsche Fassung EN 16714-1:2016*, DIN EN 16714-1, DIN Deutsches Institut für Normung e. V., Berlin, Nov. 2016.

[18] B. Zhang *et al.,* "Detection of Subsurface Defect for Metal Additive Manufacturing Using Flash Thermography," in *2018 ASPE and euspen Summer Topical Meeting on Advancing Precision in Additive Manufacturing*, American Society for Precision Engineering (ASPE), Ed., Berkeley, California, USA, 2018, pp. 121–126.

[19] B. Zhang *et al.,* "A Flash Thermography Technique for In Situ Inspection for the Laser Powder Bed Fusion Process," pp. 170–177, 2018.

[20] I. Yadroitsev, P. Krakhmalev, and I. Yadroitsava, "Selective laser melting of Ti6Al4V alloy for biomedical applications: Temperature monitoring and microstructural evolution," *Journal of Alloys and Compounds*, vol. 583, pp. 404–409, 2014.

[21] M. A. Doubenskaia *et al.,* "Determination of True Temperature in Selective Laser Melting of Metal Powder Using Infrared Camera," *MSF*, vol. 834, pp. 93–102, 2015.

[22] B. Lane *et al.,* "Thermographic Measurements of the Commercial Laser Powder Bed Fusion Process at NIST," *Rapid Prototyping Journal*, vol. 22, no. 5, pp. 778–787, 2016.

[23] F. Herzer *et al.,* "Detection of Defects in Solidified Layers within Laser-based Powder Bed Fusion using Active Thermography," *Procedia CIRP*, vol. 104, no. 4, pp. 518–523, 2021.